Available online at www.sciencedirect.com
ScienceDirect
Journal of Power Sources 163 (2006) 523–531
JOURNAL OF POWER SOURCES
www.elsevier.com/locate/jpowsour

Dynamic modeling of a hybrid system of the solid oxide fuel cell and recuperative gas turbine

Xiongwen Zhang, Jun Li, Guojun Li *, Zhenping Feng

School of Energy and Power Engineering, Xi'an Jiaotong University, Shaanxi, China

Received 12 July 2006; received in revised form 2 September 2006; accepted 15 September 2006
Available online 30 October 2006

Abstract

The hybrid solid oxide fuel cell (SOFC) and gas turbine (GT) system is a promising concept in the future power generation for its high-performance and low-emission. The dynamic model for the hybrid system of integrated SOFC and recuperative GT with air reheating component is presented in this work. A dynamic model was put forward based on the conservation equations of mass, energy and force through the whole plant, with specific source terms in different types of components. The SOFC was modeled on the basis of the Exponential Decay function and the Exponential Associate function, which describe the characteristics of the parameters distribution within the SOFC. A cubic curve was employed to denote the compressor pressure characteristics. In the turbine model, the relation between the work done and the inlet condition of turbine was determined according to the turbine nozzle work characteristics. The developed system model was programmed and implemented in the simulation tool Aspen Custom Modeler. The current density of SOFC was selected as disturbance variable during the dynamic simulation using the developed dynamic model. The responses of the SOFC air inlet temperature, SOFC outlet temperature, and turbine inlet temperature, the output voltage, and the gas species molar fractions at the outlet of SOFC were presented. The obtained results show that the presented dynamic model can be able to simulate the system dynamic track reasonably.

Keywords: Solid oxide fuel cell; Hybrid system; Dynamic model

1. Introduction

The hybrid solid oxide fuel cell (SOFC) and gas turbine (GT) system is a promising concept in the future power generation for its high-performance and low-emission. The interest in the hybrid system has been increasing with the improvement of GT technologies and maturity of modular fuel cell in recent years, leading to the fact that the high-performance hybrid cycle can be applied in small-capacity power systems. A research project Vision 21 program [1] was issued by the United States Department of Energy in 1997 for conceptual feasibility studies of high-efficiency fossil power plants, which aimed to develop the core modules for a fleet of fuel-flexible, multi-product energy plants with the power efficiency higher than 75% for the gas-fueled. The integration of fuel cell and GT hybrid systems was considered to be the key technology to achieve the Vision 21st goals due to its high-performance and low-emission. Siemens-Westinghouse Power Corporation has issued several conceptual design of pressurized SOFC/GT hybrid system [2]. The first demonstration project of a pressurized SOFC/GT hybrid system provided by Siemens-Westinghouse Power Corporation was carried out successfully at the University of California-Irvine. Furthermore, Allison Engine Company evaluated a pressurized SOFC coupled with conventional GT technology plant. The system was designed to operate at a pressure of 7 atm and the process showed that 67% efficiency was reached for power generation. An efficiency of 70% was deemed achievable with the improvement in component design. The cost of electricity (COE) was predicted to be comparable to the alternatives of current. Besides, NO*x* emission was less than 1 ppm [3]. In addition, McDermott Technology developed a conceptual design of a high efficiency power plant system which joined the planar SOFC technology with microturbine technology together in a combined cycle. The system was operated at atmospheric conditions while the output of the combined cycle for the power plant achieves 700 kW. The results indicated that 70% efficiency was

* Corresponding author. Tel.: +86 29 82668728; fax: +86 29 82665062.
E-mail address: liguojun@mail.xjtu.edu.cn (G. Li).

0378-7753/$ – see front matter © 2006 Elsevier B.V. All rights reserved.
doi:10.1016/j.jpowsour.2006.09.007

Nomenclature

a_0, a_1, a_2 the fitting function coefficient of specific heat capacity ($J\,mol^{-1}\,K^{-1}$)
A area (m^2)
A_1, A_2 the parameter of exponential fitting function
C_d coefficient of discharge
C_p specific heat capacity at constant pressure ($J\,kg^{-1}\,K$)
E_A activation energy ($J\,mol^{-1}$)
E_n theoretical Nernst potential (V)
f_{gw} molar ratio of methane to water
f_{reform} the reforming reaction balance constant
F Faraday constant (=96,485 $C\,mol^{-1}$), force (N)
h specific enthalpy ($J\,kg^{-1}$)
Δh change of specific enthalpy ($J\,kg^{-1}$)
H parameter of formula (9)
i current density ($A\,m^{-2}$)
i_L diffusion limiting current density ($A\,m^{-2}$)
i_0 exchange current density ($A\,m^{-2}$)
k specific kinetic energy ($J\,kg^{-1}$)
k_{reform} reforming chemical reaction constant (=4274 $mol\,s^{-1}\,m^{-2}\,bar^{-1}$)
k_{shift} shift gas–water chemical reaction constant (=$1.2 \times 104\,mol\,m^{-3}\,s^{-1}$)
K equilibrium constant
$\dot{m}$ mass flow ($kg\,s^{-1}$)
M molecular mass ($kg\,mol^{-1}$)
n molar weight (mol)
$\dot{n}$ molar flow ($mol\,s^{-1}$)
n_e electrons transferred per reaction
p operating pressure (Pa)
$p_{reference}$ reference pressure (Pa)
p_0 standard pressure (Pa)
q chemical reaction heat ($J\,mol^{-1}$)
$Q_{exchange}$ exchanged heat ($J\,s^{-1}$)
Q_{gen} generated heat ($J\,s^{-1}$)
R molar universal gas constant (=8.314 $J\,mol^{-1}\,K^{-1}$), chemical reaction rate ($mol\,s^{-1}$)
R_e electrolyte ohmic resistance (Ω)
R_g mass universal gas constant ($J\,kg^{-1}\,K^{-1}$)
S_m mass source ($kg\,s^{-1}$)
S_n species molar source ($mol\,s^{-1}$)
S_q heat source ($J\,s^{-1}$)
S_w work done (W)
t time (s)
t_1, t_2 fitting function exponential parameter
T temperature (K)
u impeller tip velocity ($m\,s^{-1}$)
U voltage (V)
v fluid velocity ($m\,s^{-1}$)
V volume (m^3)
W parameter of formula (9)
x gaseous molar fraction
y fitting function
z dimensionless spatial coordinate of gas flow direction ($z \in [0,1]$)

Greek letters
γ ratio of specific heat
δ thickness of housing for control volume (m)
ε heat exchanger effectiveness
θ turbine flow factor
λ stoichiometric reaction coefficient
ξ splitter diffluent factor
π turbine work done factor
ρ density ($kg\,m^{-3}$)
ϕ mass flow coefficient
χ corrected coefficient of Eq. (3)
ψ, ψ_0 isentropic work coefficient

Subscripts
active chemical active
av average
cold cold side control volume
CH_4 methane
CO carbon monoxide
CO_2 carbon dioxide
el electrochemical reaction
hot hot side control volume
H_2 hydrogen
H_2O water (gas)
i index of the control volume
imp impeller
isen isentropic
j index of gaseous species
k index of anabranch flow
nozzle turbine nozzle
N_2 nitrogen
O_2 oxygen
ref reforming reaction
rot in rotating equipment
shift shift reaction
1–6 index of the chemical reactions (R1)–(R6)

Superscripts
add addition
anode anode side control volume
cathode cathode side control volume
in inlet
out outlet
s solid

possible and the COE was comparable to present day alternatives [4].

The GT is driven by employing the rejected thermal energy and residual fuel from a fuel cell in the SOFC/GT hybrid system. Fig. 1 shows a cycle scheme of SOFC/GT hybrid system with recuperative heat exchanger (RHE) as air reheater. Some models

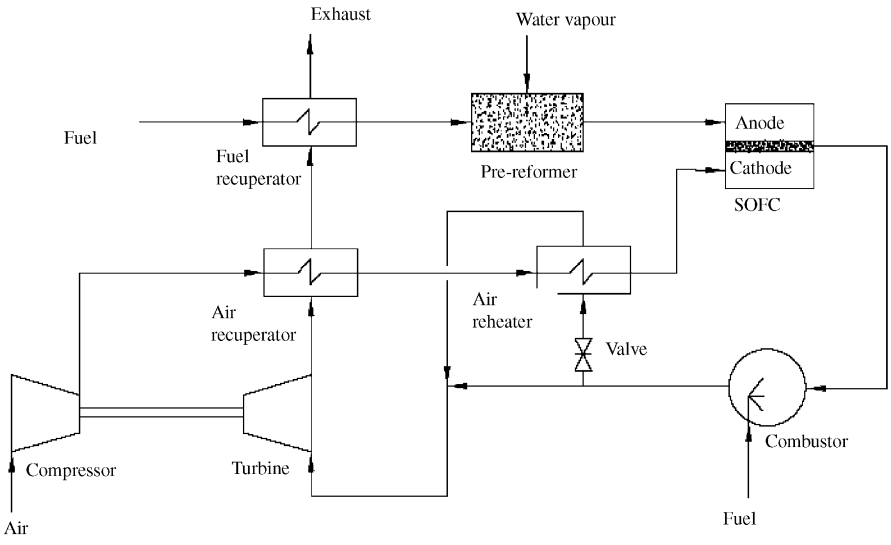

Fig. 1. Scheme of a SOFC/GT hybrid system with RHE air reheater cycle.

adapted to the cycle of hybrid system were presented in Refs. [5–8]. Most of them were developed on the basis of a steady point or a specific product for the balance of plant (BoP) of the hybrid system. The components of compressor and turbine dynamic work performance characteristics were not considered enough in the system model, as well as the spatial variation effect within the SOFC, which was not taken into account in the lumped SOFC model [9].

The aim of present work focuses on the development of a dynamic model for the SOFC/GT hybrid system. In Section 2 of this paper, we build the models based on the mass balance differential equation, energy balance differential equation and force balance equation for each of the components. Section 3 presents the dynamic simulation carried out using the developed model, which is programmed and implemented in the simulation tool Aspen Custom Modeler [10] allowing users to develop custom-made model. Then the responses of some parameters such as temperature, fuel cell output voltage and species molar fraction are analyzed while the current density of the SOFC was assumed as the disturbance variable during the simulation. A summary of the work is given in Section 4.

2. Mathematical model

Firstly, model of each component is built for the hybrid system. The most important assumptions used in present study are listed as follows: (1) one-dimensional treatment of flowpaths. All fluid properties are assumed to be uniform over any cross section because the rate of fluid properties variations perpendicular to the streamline is small compared with the rate of changes along the streamline; (2) the friction loss along the streamline is neglected; (3) both air and fuel are assumed as the ideal gas, which makes them satisfy the ideal gas state equation; (4) the difference of the fluid momentum between the inlet and the outlet for each component is neglected.

In order to make a process model be easily adapted to variation of the process, it is necessary to build a generic model. In this way, system model should be easily extended or modified such as layout schemes, components size. The control volume is defined for the place, where the gas state is varied within the component along the flowpaths. A general model for each of control volume is to be proposed, and then the specific source terms are to be determined.

The mass balance, energy balance and gas species molar balance should be satisfied within the control volume. The corresponding conservation equations are written as:

For the mass balance:

$$V_i \frac{\mathrm{d}\rho_i^{\mathrm{out}}}{\mathrm{d}t} = \dot{m}_i^{\mathrm{in}} - \dot{m}_i^{\mathrm{out}} + S_{\mathrm{m}i} \tag{1}$$

where S_{m} is the term of mass source for the control volume.

For the energy balance:

$$[\rho_i^{\mathrm{s}} V_i^{\mathrm{s}} C_{pi}^{\mathrm{s}} + V_i \rho_i^{\mathrm{out}} (C_{pi}^{\mathrm{out}} - R_{\mathrm{g}i}^{\mathrm{out}})] \frac{\mathrm{d}T_i^{\mathrm{out}}}{\mathrm{d}t} = \dot{m}_i^{\mathrm{in}} (h_i^{\mathrm{in}} + k_i^{\mathrm{in}}) - \dot{m}_i^{\mathrm{out}} (h_i^{\mathrm{out}} + k_i^{\mathrm{out}}) + S_{\mathrm{q}i} + S_{\mathrm{w}i} \tag{2}$$

where S_{q} is the heat source and S_{w} is the work done for the control volume. The gas mass constant R_{g} is obtained according to the composition of the gas mixture. The specific heat at constant pressure is assumed quadratic relation with temperature. The term $\rho_i^{\mathrm{s}} V_i^{\mathrm{s}} C_{pi}^{\mathrm{s}}$ represent the housing thermal capacity of the control volume. In this paper, the material of the control volume housing is assumed to be Ferro and the control volume is assumed to be tetragonal volume. Then the solid volume of housing can be estimated according to the follow equation:

$$V_i^{\mathrm{s}} = 6\chi\delta V_i^{2/3} \tag{3}$$

where δ denotes the thickness of the control volume housing. The coefficient χ is introduced for considering the control volume that may be includes solid component. The fuel cell stack thermal capacity is calculated according to the single-unit cell geometry parameters, the total active area, and the heat properties of electrode, electrolyte and connector.

For each of gas species molar balance equations

$$\frac{\mathrm{d}n_{ij}^{\mathrm{out}}}{\mathrm{d}t} = \dot{n}_i^{\mathrm{in}} x_{ij}^{\mathrm{in}} - \dot{n}_i^{\mathrm{out}} x_{ij}^{\mathrm{out}} + S_{\mathrm{n}_{ij}} \tag{4}$$

where S_{n} is species molar source for the control volume. Molar weight n_{ij} satisfies ideal gas equation of state. The force balance is assumed for each of the control volume, then, we get

$$p_i^{\mathrm{in}} A_i^{\mathrm{in}} - p_i^{\mathrm{out}} A_i^{\mathrm{out}} + F_{\mathrm{friction}\,i} + F_{\mathrm{rot}\,i} + F_{\mathrm{areachange}\,i} = 0 \tag{5}$$

The friction force is negligible according to the assumption (2). $F_{\mathrm{areachange}\,i}$ is the force produced by the pressure effect in case of the variation of the cross section area along the flow direction within the control volume. The flowing area is assumed as constant within the control volume in this study. Then Eq. (5) is simplified as follows

$$A_i(p_i^{\mathrm{in}} - p_i^{\mathrm{out}}) + F_{\mathrm{rot}\,i} = 0 \tag{6}$$

where F_{rot} is the force on the fluid in the control volume. In this paper, it was calculated only in compressor and turbine components in the hybrid system.

2.1. Compressor model

In order to simulate the compressor behavior, relations have to be found among the source terms (forces on, heat transport to, and work done on the fluid), inlet condition, mass flow, speed and geometry of compressor. The fluid isentropic enthalpy rise is first determined according to the flow coefficient. The flow coefficient is defined as:

$$\phi = \frac{v^{\mathrm{in}}}{u} \tag{7}$$

The fluid isentropic enthalpy rise is non-dimensionalized through division by the square impeller tip velocity:

$$\psi = \frac{\Delta h_{\mathrm{isen}}}{\rho u^2} \tag{8}$$

A cubic relation between the fluid isentropic enthalpy rise and the flow coefficient is adopted according to the work of Moore [11]. Fig. 2 shows one such curve used in this paper. The formula of the cubic curve is

$$\psi(\phi) = \psi_0 + H\left[1 + \frac{3}{2}\left(\frac{\phi}{W} - 1\right) - \frac{1}{2}\left(\frac{\phi}{W} - 1\right)^3\right] \tag{9}$$

where the parameters ψ_0, H, and W are illustrated in Fig. 2. The isentropic enthalpy rise Δh_{isen} is obtained through Eqs. (8) and (9). Then the force F_{rot} on the gas in the impeller for force balance Eq. (6) are calculated from Δh_{isen} using

$$\frac{p^{\mathrm{in}} + F_{\mathrm{rot}}/A_{\mathrm{imp\,av}}}{p^{\mathrm{in}}} = \left(\frac{T^{\mathrm{in}} + \Delta h_{\mathrm{isen}}/C_{\mathrm{p}}}{T^{\mathrm{in}}}\right)^{\gamma/(\gamma-1)} \tag{10}$$

Then

$$S_{\mathrm{w}} = \dot{m}^{\mathrm{in}} \Delta h_{\mathrm{isen}} \tag{11}$$

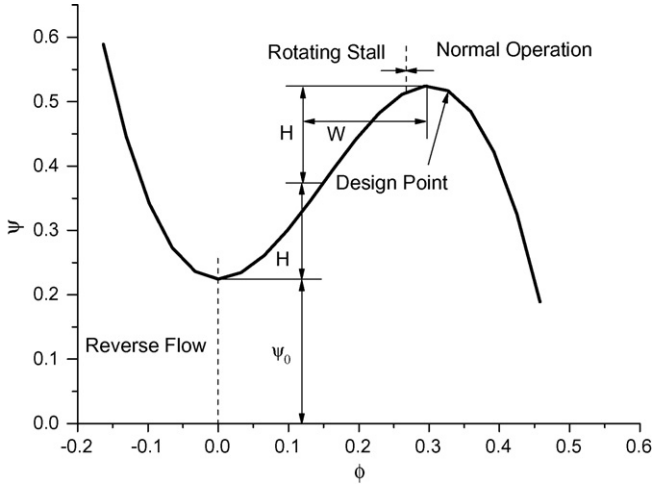

Fig. 2. Typical compressor enthalpy rises [11].

2.2. Turbine model

Like the approach taken to formulate and construct the compressor model, turbine force and work are also determined from a set of turbine performance characteristics. To describe the turbine performance characteristics, two parameters are defined—turbine flow factor, θ, and turbine work done factor, π,

$$\theta = \frac{\dot{m}^{\mathrm{in}}\sqrt{T^{\mathrm{in}}}}{p^{\mathrm{in}}} \tag{12}$$

$$\pi = \frac{-\Delta h_{\mathrm{isen}}}{T^{\mathrm{in}}} \tag{13}$$

A typical turbine performance curve [12] is drawn in Fig. 3. In this paper, the turbine nozzle area is set to be a variable, and then the expansion ratio of the turbine is modified by changing the nozzle area. Assuming the expansion ratio at the nozzle choke condition is known, we can obtain the value of π_{choke} based on the assumption of isentropic process for the turbine. The choke

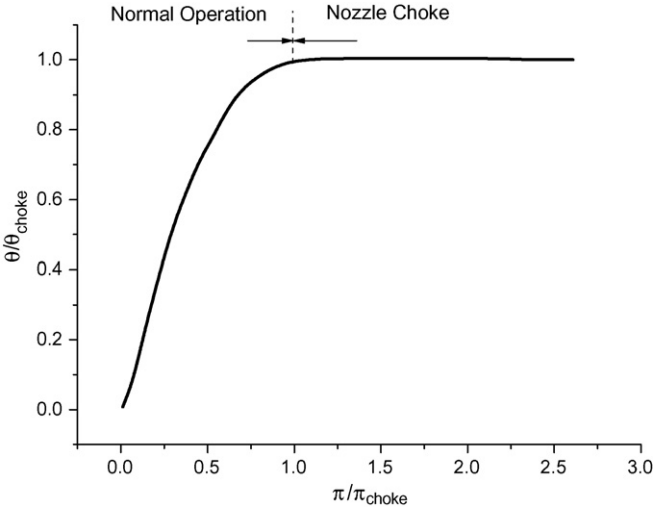

Fig. 3. Typical turbine performance curves [12].

flow of the turbine nozzle is calculated by the following equation:

$$\dot{m}_{\text{choke}} = C_{\text{d}} A_{\text{nozzle}} p^{\text{in}} \sqrt{\frac{\gamma}{RT^{\text{in}}} \left(\frac{2}{\gamma+1}\right)^{(\gamma+1)/(\gamma-1)}} \tag{14}$$

The turbine flow factor is determined from the inlet condition according to Eq. (12). Then, the work done factor π is calculated based on the turbine performance curve. The source of output power becomes:

$$S_{\text{w}} = \pi \dot{m}^{\text{in}} T^{\text{in}} \tag{15}$$

The force produced by gas fluid on the rotor is expressed with Eq. (10), in which the enthalpy change term is calculated from the work done factor.

2.3. SOFC model

A planar SOFC developed by International Energy Agency (IEA) [13,14] was used to be combined with GT in this study. The electrochemical reaction formula for the planar SOFC is

$$(1/2)\text{O}_2 + \text{H}_2 \rightarrow \text{H}_2\text{O} \tag{R1}$$

For the internal reforming of presently used SOFC, the reforming reaction and gas–shift reaction are included in the model:

$$\text{Steam-reforming}: \ \text{CH}_4 + \text{H}_2\text{O} \rightarrow \text{CO} + 3\text{H}_2 \tag{R2}$$

$$\text{Shifting}: \ \text{CO} + \text{H}_2\text{O} = \text{CO}_2 + \text{H}_2 \tag{R3}$$

The geometry parameters and the design operating condition of the SOFC were given in Ref. [14]. A mathematic model was presented in [9], which employed two fitting functions—the Exponential Decay function and the Exponential Associate function to describe the characteristics of the gaseous molar fraction and temperature distribution in the flow direction in the SOFC. The fitting functions were expressed as:

$$y = \begin{cases} y_0 + (A_0 \text{e}^{-(z/t_1)} + A_2 \text{e}^{-(z/t_2)}) \text{ for the Exponential Decay function} \\ y_0 + [A_0(1 - \text{e}^{-(z/t_1)}) + A_2(1 - \text{e}^{-(z/t_2)})] \text{ for the Exponential Associate function} \end{cases} \tag{16}$$

where y denotes the gaseous molar fraction and the temperature, which is a function of the dimensionless spatial coordinate of gas flow direction z. The parameters of t_1, t_2, y_0, A_1, A_2 are determined according to the method from Ref. [9].

In order to model the sources of the energy balance equation, mass balance equation, and gas species balance equations, the rate of the electrochemical reaction, the reforming reaction and the water–gas shift reaction should be known. The electrochemical reaction rate is defined as

$$R_{\text{el}} = A_{\text{active}} \frac{i}{n_{\text{e}} F} \tag{17}$$

The reforming reaction rate is

$$R_{\text{ref}} = A_{\text{ref}} k_{\text{reform}} f_{\text{reform}} \, p \int_0^1 x_{\text{CH}_4} \exp\left(-\frac{E_{\text{A}}}{RT}\right) \text{d}z \tag{18}$$

where x_{CH_4}, T are the functions of z satisfying the formulations (16). The water–gas shift reaction is given as follows

$$R_{\text{shift}} = A_{\text{shift}} k_{\text{shift}} \, p \int_0^1 (x_{\text{CO}} x_{\text{H}_2\text{O}} - K_{\text{shift}} x_{\text{CO}_2} x_{\text{H}_2}) \, \text{d}z \tag{19}$$

where K_{shift} is obtained using the method in Ref. [15]. The sources of the mass, the species molar, and the energy balance equations are calculated, respectively with

$$S_{\text{m}}^{\text{anode}} = -M_{\text{O}_2} \lambda_{\text{O}_2,1} R_{\text{el}} \tag{20}$$

$$S_{\text{m}}^{\text{cathode}} = M_{\text{O}_2} \lambda_{\text{O}_2,1} R_{\text{el}} \tag{21}$$

$$S_{\text{n},j}^{\text{anode}} = \lambda_{j,1} R_{\text{el}} + \lambda_{j,2} R_{\text{ref}} + \lambda_{j,3} R_{\text{shift}} \tag{22}$$

$$S_{\text{n},j}^{\text{cathode}} = \lambda_{j,1} R_{\text{el}} \tag{23}$$

$$S_{\text{q}}^{\text{anode}} = \frac{C_p^{\text{anode}} \dot{m}^{\text{anode}}}{C_p^{\text{anode}} \dot{m}^{\text{anode}} + C_p^{\text{cathode}} \dot{m}^{\text{cathode}}} Q_{\text{gen}} \tag{24}$$

$$S_{\text{q}}^{\text{cathode}} = \frac{C_p^{\text{cathode}} \dot{m}^{\text{cathode}}}{C_p^{\text{anode}} \dot{m}^{\text{anode}} + C_p^{\text{cathode}} \dot{m}^{\text{cathode}}} Q_{\text{gen}} \tag{25}$$

where j denotes H_2, H_2O, CO, CO_2, CH_4 for anode side and O_2 for cathode side. And the released heat of chemical reaction is calculated according to the following formula:

$$Q_{\text{gen}} = (q_{\text{el}} R_{\text{el}} - UiA_{\text{active}}) + q_{\text{ref}} R_{\text{ref}} + q_{\text{shift}} R_{\text{shift}} \tag{26}$$

The Nernst potential is calculated as a function of current density, operating pressure, temperature and the gaseous molar fraction. The irreversibility in the voltage drop is contributed by three kinds of polarization losses, i.e. activation, concentration and ohmic overpotentials. The Nernst equation for the SOFC is:

$$E_{\text{n}} = \frac{RT}{n_{\text{e}} F} \ln K(T) - \frac{RT}{2n_{\text{e}} F} \ln\left(\frac{x_{\text{H}_2\text{O}}^2 p_0}{x_{\text{H}_2}^2 x_{\text{O}_2}}\right) \tag{27}$$

where the assumption $p^{\text{anode}} = p^{\text{cathode}} = p$ is proposed. The output voltage can be obtained through Eq. (27) subtracting the electrochemical losses

$$U = \int_0^1 \left[E_{\text{n}} - iR_{\text{e}}(T) - \frac{2RT}{n_{\text{e}} F} \sinh^{-1}\left(\frac{i}{2i_0^{\text{anode}}}\right) - \frac{2RT}{n_{\text{e}} F} \sinh^{-1}\left(\frac{i}{2i_0^{\text{cathode}}}\right) + \frac{RT}{n_{\text{e}} F} \ln\left(1 - \frac{i}{i_{\text{L}}}\right) \right] \text{d}z \tag{28}$$

where the second term on the right hand side of the above equation represents ohmic loss, the third term is the activation loss

at the anode side, the fourth term is the activation loss at the cathode side, and the last term is the concentration loss. The exchange current density is modeled in the following [16]:

$$i_0^{\text{anode}} = \gamma^{\text{anode}} \left(\frac{p^{\text{anode}} x_{\text{H}_2}}{p_{\text{reference}}} \right) \left(\frac{p^{\text{anode}} x_{\text{H}_2\text{O}}}{p_{\text{reference}}} \right) \exp\left(-\frac{E_{\text{A}}^{\text{anode}}}{RT} \right) \tag{29}$$

$$i_0^{\text{cathode}} = \gamma^{\text{cathode}} \left(\frac{p^{\text{cathode}} x_{\text{O}_2}}{p_{\text{reference}}} \right)^{0.25} \exp\left(-\frac{E_{\text{A}}^{\text{cathode}}}{RT} \right) \tag{30}$$

2.4. Pre-reformer model

The reforming reaction and water–gas shift reaction are included in the pre-reformer. The formulas of the reforming reaction rate and the shift reaction rate are obtained according to Eqs. (18) and (19) with no integration. The source term of mass balance equation equals to the needed water, which is added to ensure the reforming reaction proceeding. Then

$$S_{\text{m}} = \left(\frac{\dot{n}^{\text{in}} x_{\text{CH}_4}^{\text{in}}}{f_{\text{gw}}} - \dot{n}^{\text{in}} x_{\text{H}_2\text{O}}^{\text{in}} \right) M_{\text{H}_2\text{O}} \tag{31}$$

where f_{gw} is the molar ratio of methane to water. For the species molar fraction balance equations, there have

$$S_{\text{n},j} = \lambda_{j,2} R_{\text{ref}} + \lambda_{j,3} R_{\text{shift}} \tag{32}$$

where j denotes H_2, CO, CO_2, CH_4. The added water should be considered in the water conservation equation:

$$S_{\text{n,H}_2\text{O}} = \lambda_{\text{H}_2\text{O},2} R_{\text{ref}} + \lambda_{\text{H}_2\text{O},3} R_{\text{shift}} + \frac{\dot{n}^{\text{in}} x_{\text{CH}_4}^{\text{in}}}{f_{\text{gw}}} - \dot{n}^{\text{in}} x_{\text{H}_2\text{O}}^{\text{in}} \tag{33}$$

The additional heat is needed because of the endothermic reforming reaction. Therefore,

$$S_{\text{q}} = q_{\text{ref}} R_{\text{ref}} + q_{\text{shift}} R_{\text{shift}} + S_{\text{m}} h_{\text{H}_2\text{O}}^{\text{add}} \tag{34}$$

2.5. Combustor model

In the combustor the combustion of the exhaust hydrogen and carbon monoxide from fuel cell should be taken into account. The additional fuel is added to control the turbine inlet temperature. Three oxidation reactions exist in the combustor:

$$\text{CH}_4 + 2\text{O}_2 = 2\text{H}_2\text{O} + \text{CO}_2 \tag{R4}$$

$$\text{CO} + 0.5\text{O}_2 = \text{CO}_2 \tag{R5}$$

$$\text{H}_2 + 0.5\text{O}_2 = \text{H}_2\text{O} \tag{R6}$$

The source of mass balance equation is exactly equal to the fuel added. Here we assume the combustor efficiency to be constant and equal to 100%. Then we obtain:

$$S_{\text{n}j} = \lambda_{j,4}(\dot{n}_{\text{CH}_4}^{\text{in}} x_{\text{CH}_4}^{\text{in}} + \dot{n}_{\text{CH}_4}^{\text{fuel}} x_{\text{CH}_4}^{\text{fuel}}) + \lambda_{j,5}(\dot{n}_{\text{CO}}^{\text{in}} x_{\text{CO}}^{\text{in}} + \dot{n}_{\text{CO}}^{\text{fuel}} x_{\text{CO}}^{\text{fuel}}) + \lambda_{j,6}(\dot{n}_{\text{H}_2}^{\text{in}} x_{\text{H}_2}^{\text{in}} + \dot{n}_{\text{H}_2}^{\text{fuel}} x_{\text{H}_2}^{\text{fuel}}) \tag{35}$$

The heat added to the energy equation is given as

$$S_{\text{q}} = q_{\text{CH}_4}(\dot{n}_{\text{CH}_4}^{\text{in}} x_{\text{CH}_4}^{\text{in}} + \dot{n}_{\text{CH}_4}^{\text{fuel}} x_{\text{CH}_4}^{\text{fuel}}) + q_{\text{CO}}(\dot{n}_{\text{CO}}^{\text{in}} x_{\text{CO}}^{\text{in}} + \dot{n}_{\text{CO}}^{\text{fuel}} x_{\text{CO}}^{\text{fuel}}) + q_{\text{H}_2}(\dot{n}_{\text{H}_2}^{\text{in}} x_{\text{H}_2}^{\text{in}} + \dot{n}_{\text{H}_2}^{\text{fuel}} x_{\text{H}_2}^{\text{fuel}}) \tag{36}$$

2.6. Heat exchanger model

The model of heat exchanger consists of two control volumes—a cold flow and a hot flow. The heat exchange between the two flows is calculated using a given recuperator effectiveness [17]:

$$Q_{\text{exchange}} = \varepsilon \min(C_{\text{p cold}}^{\text{in}} \dot{m}_{\text{cold}}^{\text{in}}, C_{\text{p hot}}^{\text{in}} \dot{m}_{\text{hot}}^{\text{in}})(T_{\text{hot}}^{\text{in}} - T_{\text{cold}}^{\text{in}}) \tag{37}$$

In this work ε is set to be 0.85. The source of energy equation then becomes

$$S_{\text{q cold}} = Q_{\text{exchange}} \tag{38}$$

$$S_{\text{q hot}} = -Q_{\text{exchange}} \tag{39}$$

2.7. Mixer model

For the case of two streams or multi-stream confluence, the maximal mass stream is defined as mainstream, which satisfies the balance equation. The anabranch flows are specified as the sources of mainstream. The force on the mainstream by the anabranch flow is assumed to be zero in the mainstream flow direction. Then

$$S_{\text{m}} = \sum_k \dot{m}_k^{\text{in}} \tag{40}$$

$$S_{\text{n}i} = \sum_k (\dot{n}_k^{\text{in}} x_{k,i}^{\text{in}}) \tag{41}$$

$$S_{\text{q}} = \sum_k \sum_i (\dot{n}_k^{\text{in}} x_{k,i}^{\text{in}} h_{k,i}^{\text{in}}) \tag{42}$$

where the subscripts k, i denote the index of anabranch and gas species, respectively.

2.8. Splitter model

Like the confluence mixture model, a maximal mass anabranch flow is defined as the mainstream. A variable named diffluence factor is first proposed to control the corresponding anabranch mass flow, which is defined as

$$\xi_k = \frac{\dot{m}_k^{\text{out}}}{\dot{m}^{\text{in}}} \tag{43}$$

Then the sources for balance equations are determined according to the following formulas:

$$S_{\text{m}} = \sum_k (-\xi_k \dot{m}^{\text{in}}) \tag{44}$$

$$S_{\text{n}i} = \sum_k (-\xi_k \dot{n}_k^{\text{in}} x_{k,i}^{\text{in}}) \tag{45}$$

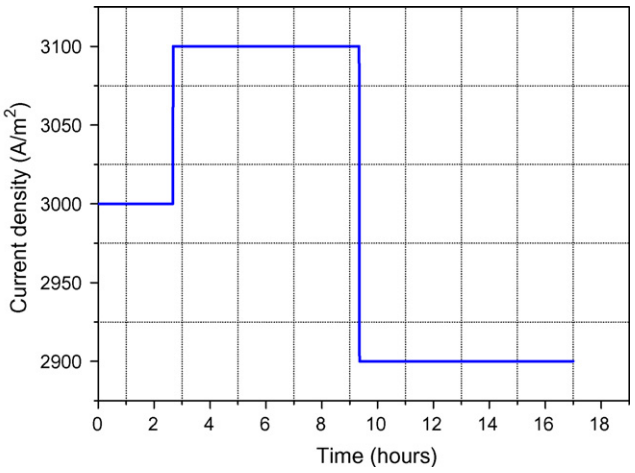

Fig. 4. Disturbance course of current density.

$$S_q = \sum_k \sum_i (-\xi_k \dot{n}_k^{in} x_{k,i}^{in} h_{k,i}^{in}) \quad (46)$$

where the subscripts k, i denote the index of anabranch and gas species, respectively.

3. Dynamic simulation

A planar SOFC presented by IEA is adopted as the simulation case in this work. The geometry parameters of the single-unit cell are given as follows: active area 5.42 mm × 100 mm, anode thickness 50 μm, cathode thickness 50 μm, electrolyte thickness 150 μm, channel height 1 mm, rib width 2.42 mm, and bipolar plate thickness 2.5 mm. The properties of electric conductivity for the electrodes and the electrolyte were specified in Ref. [13]. The mass density and heat capacity of anode, cathode, electrolyte, and connector was assumed to be 6600 kg m^{-3} and 400 J (kg K)$^{-1}$, respectively according to IEA report [13]. The fuel cell stage is composed of single-unit cells. The designed parameters of the proposed system are given in Table 1.

The simulation is carried out using the proposed model in the simulation tool Aspen Custom Modeler, which allows users to build custom-made mathematical model. All the component models are programmed with the modeling language provided by Aspen Custom Modeler programmer environment.

The current density of SOFC is selected as the disturbance during the dynamic simulation. Fig. 4 shows a specific disturbance characteristic of the current density. The fuel mass flow

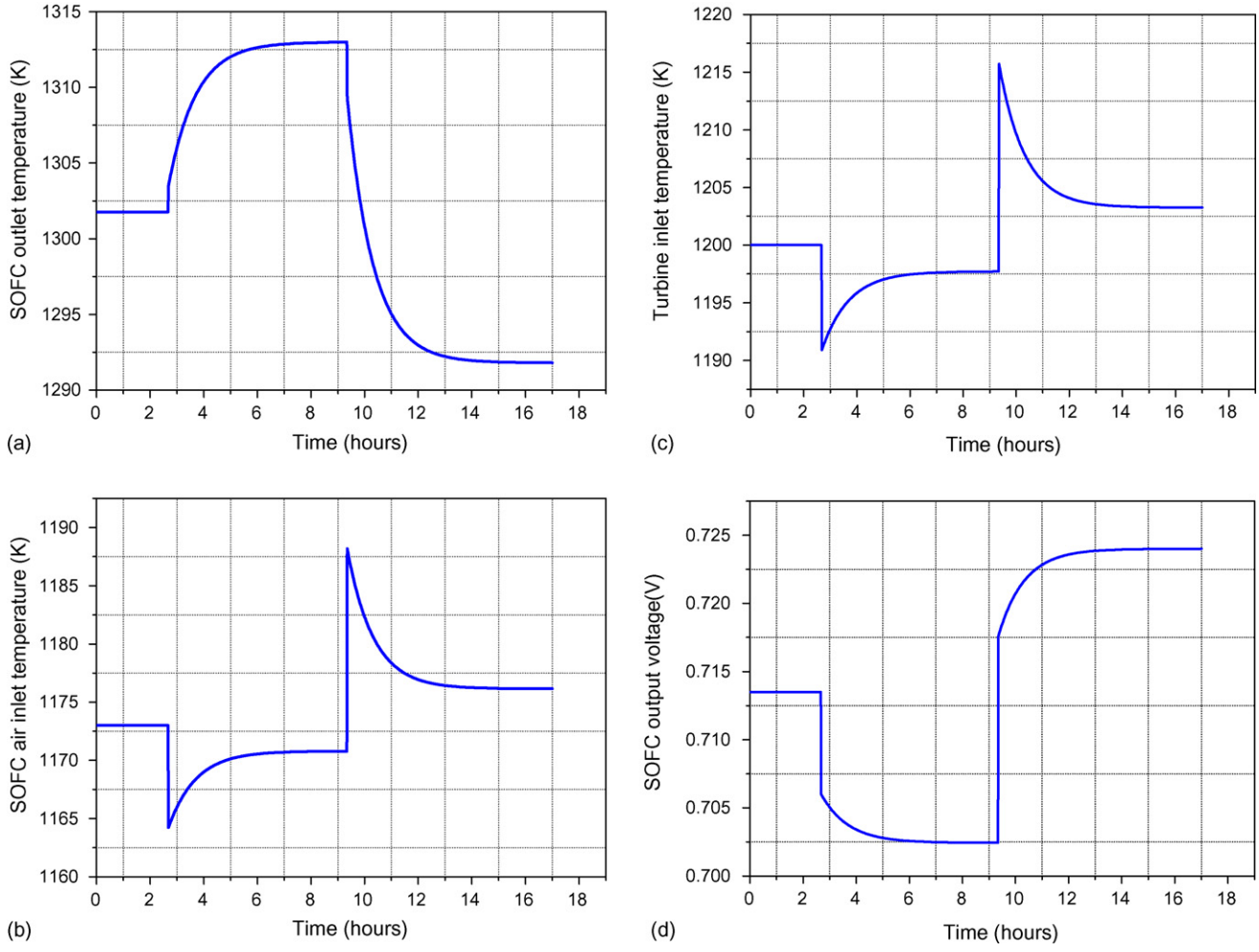

Fig. 5. Response of temperature and output voltage: (a) SOFC outlet temperature; (b) SOFC air inlet temperature; (c) turbine inlet temperature; (d) SOFC output voltage.

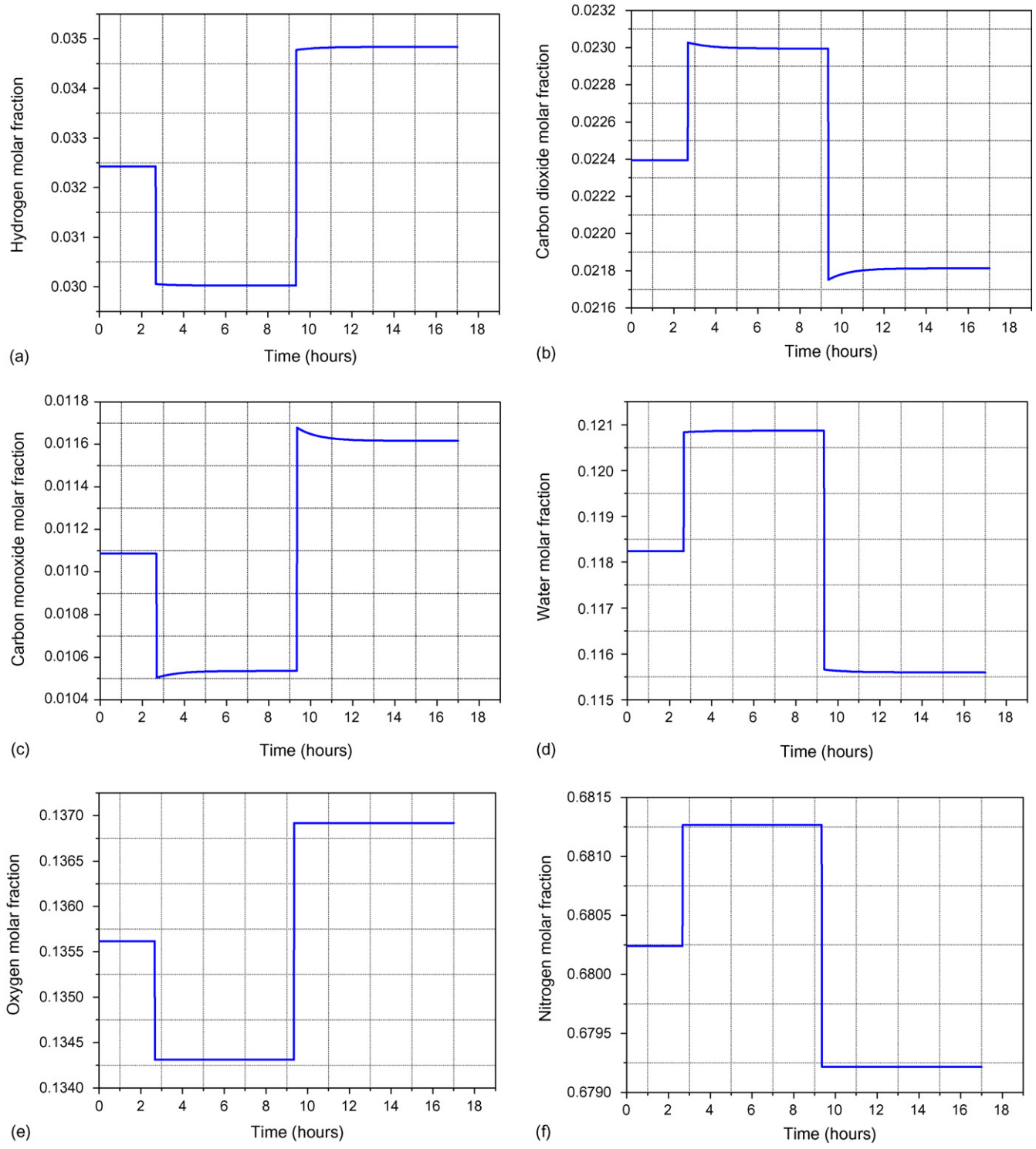

Fig. 6. Response of the gases species molar fraction after the fuel cell: (a) H_2; (b) CO_2; (c) CO; (d) H_2O; (e) O_2; (f) N_2.

and air mass flow of fuel cell are assumed to be fixed during the simulation. Steady simulation is first implemented at the design point. Then the dynamic mode is set and the simulation is run at the design operating condition, in which the current density equals to 3000 A m^{-2}. The current density jumps up to the level of 3100 A m^{-2} firstly and then down to 2900 A m^{-2} after a few hours according to Fig. 4.

In Fig. 5 the responses of temperature are presented, including the temperature of SOFC air inlet (a), SOFC outlet (b) and the turbine inlet (c). The polarization losses of SOFC are positively correlated with current density [18]. Therefore, the released heat increases as current density rises. Then as shown in Fig. 5(b), the response curve of SOFC outlet temperature changes as the same direction with current density disturbance. However, the fuel

Table 1
Assumed system components performance

Compressor	Isentropic efficiency	85%
	Inlet air pressure (Pa)	101,325
	Inlet air temperature (K)	298
	Inlet air composition	O_2: 21%, N_2: 79%
	Shaft speed (rpm)	46,000
	Pressure ratio	5.157
Turbine	Isentropic efficiency	85%
	Inlet gas temperature (K)	1200
	Expansion ratio	4.55
SOFC	Fuel utilization	85%
	Air utilization	25%
	Current density (A m^{-2})	3000
	Inlet temperature (K)	1173
Combustor	Efficiency	100%
Heat exchanger	Effectiveness	85%
Pre-reformer	Steam/methane ratio	2.5
	Operating temperature (K)	1173
	Inlet fuel composition	100% CH_4

utilization decreases with increasing of current density when the fuel mass flow is set to be fixed. In the other words, the residual fuel from the exhaust of SOFC that is combusted in the combustor to raise the mixture gas temperature decreases as current density rise. So the turbine inlet temperature and the air inlet temperature of SOFC are negatively correlated with current density. It can be seen that the track of above three temperature variations due to the current density disturbance is simulated reasonably. Fig. 5(d) shows the response of the output voltage of the SOFC, which increases with the decrease of the current density.

Fig. 6 shows the responses of the SOFC outlet gaseous molar fraction. The responses of each of the species molar fraction are much faster than that of temperature. The steady value of the carbon dioxide, water and nitrogen molar fractions are in proportion to the current density while the variations of hydrogen, oxygen and carbon monoxide molar fraction go in the opposite change direction of the current density. From Fig. 6(b) and (c), we can find that the fluctuating direction of the carbon dioxide molar fraction around the steady value at the jump point is inversed with that of carbon dioxide molar fraction. This is due to the fact that the shift reaction is closely related with temperature. The shift reaction shows more negative direction as the operating temperature of SOFC increases. So the molar fractions of reactant species CO increase and the product species CO_2 decrease if the temperature rises.

4. Conclusion

A dynamic model of the SOFC combined with recuperative gas turbine hybrid system has been developed. Dynamic simulation for the proposed hybrid system was implemented based on the developed model, which was programmed via the simulation tool Aspen Custom Modeler. The current density of the SOFC was selected as disturbance variable in the simulation. The fuel and air mass flows were fixed and the fuel utilization and air utilization were specified as free variables during the simulation. Dynamic simulation results show that the SOFC outlet temperature was positively related with current density while was inversed for SOFC air inlet temperature and turbine inlet temperature. The response time constant of the species molar fraction is much smaller than that of temperature. Simulation results show that the developed model can follow the track of the disturbance very well.

Acknowledgement

This study was financially supported by the Doctor Foundation of Xi'an Jiaotong University (No. DFXJTU2005-01).

References

[1] J.P. Strakey, Presented at Advanced Coal-Based Power and Environmental Systems '98 Conference, Morgantown, WV, 1998.
[2] S.E. Veyo, L.A. Shockling, J.T. Dederer, J.E. Gillett, W.L. Lundberg, ASME J. Eng. Gas Turb. Power 124 (2002) 845–849.
[3] EG & G Technical Services, Inc. Science Applications International Corporation, Fuel Cell Handbook, 6th ed., U.S. Department of Energy Office of Fossil Energy, National Energy Technology Laboratory, West Virginia, 2002.
[4] L.J. Chaney, M.R. Tharp, T.W. Wolf, T.A. Fuller, J.J. Hartvigson, Fuel cell/micro-turbine combined cycle, Final Report, McDermott Technology, Inc. Alliance, 1999.
[5] J. Palsson, A. Selimovil, L. Sjunnesson, J. Power Sources 86 (2000) 442–448.
[6] M. Ferrari, A. Traverso, L. Magistri, A.F. Massardo, J. Power Sources 149 (2005) 22–32.
[7] A.D. Rao, A thermodynamic analysis of tubular SOFC based hybrid systems, Ph.D. Thesis, University of California, Irvine, USA, 2001.
[8] R.A. Roberts, J. Brouwer, ASME J. Fuel Cell Sci. Technol. 3 (2006) 18–25.
[9] X. Zhang, J. Li, G. Li, Z. Feng, J. Power Sources 160 (2006) 258–267.
[10] Aspen Custom Modeler 10.1 User Manual, Sheraton House, Cambridge, MA, 1999.
[11] F.K. Moore, E.M. Greitzer, ASME Paper 85-GT-171, 1986.
[12] A.K. Owen, A. Daugherty, D. Garrard, H.C. Reynolds, R.D. Wright, ASME J. Eng. Gas Turb. Power 121 (1999) 377–383.
[13] E. Achenbach, "SOFC stack modeling", Final Report of Activity A2, Annex II: Modeling and Evaluation of Advanced Solid Oxide Fuel Cells, International Energy Agency Programme on R, D&D on Advanced Fuel Cells, Juelich, Germany, 1996.
[14] J.R. Ferguson, J.M. Fiard, R. Herbin, J. Power Sources 58 (1996) 106–122.
[15] H. Yakabe, T. Ogiwara, M. Hishinuma, I. Yasuda, J. Power Sources 102 (2001) 144–154.
[16] P. Costamagna, K. Honegger, J. Electrochem. Soc. 145 (1998) 3995–4007.
[17] Sh.M. Yang, W.Q. Tao, Heat Transfer, 3rd ed., High Education Press, 1998 (in Chinese).
[18] S.H. Chan, K.A. Khor, Z.T. Xia, J. Power Sources 93 (2001) 130–140.